Jamming of Soft Disks: Disorder, Entropy, and Athermal Statistical Mechanics

Kabir Ramola

Martin Fisher School of Physics,
Brandeis University

In collaboration with

Bulbul Chakraborty,
Stefano Martiniani,
K. Julian Schrenk,
Daan Frenkel

September 15, 2017

Granular Matter

Statistical Ensembles

- The concept of **'ensembles'** plays a key role in equilibrium statistical mechanics.
- The distinction between a liquid at thermal equilibrium and a granular material is that in a liquid, atoms undergo **thermal motion**.
- In a granular medium (in the absence of outside perturbations) the system is trapped in one of many **(very many)** local potential energy minima.
- Gibbsian statistical mechanics **cannot be used** to describe such a system.

Granular Ensembles

- Granular systems are made up of macroscopic particles and are inherrently **athermal**.
- What is the correct **statistical ensemble** for **static granular systems**?
- How does one build a **microscopic theory using local observables**?
- Edwards proposed that the collection of **all stable packings of a fixed number of particles in a fixed volume** might also play the role of an 'ensemble'. Ref: S. F. Edwards, R. B. S. Oakeshott, Physica A 157, 180 (1991).
- A statistical-mechanics like formalism would result if one assumed that all such packings were **equally likely to be observed**, once the system had settled into a mechanically stable 'jammed' state.

Jammed Packings

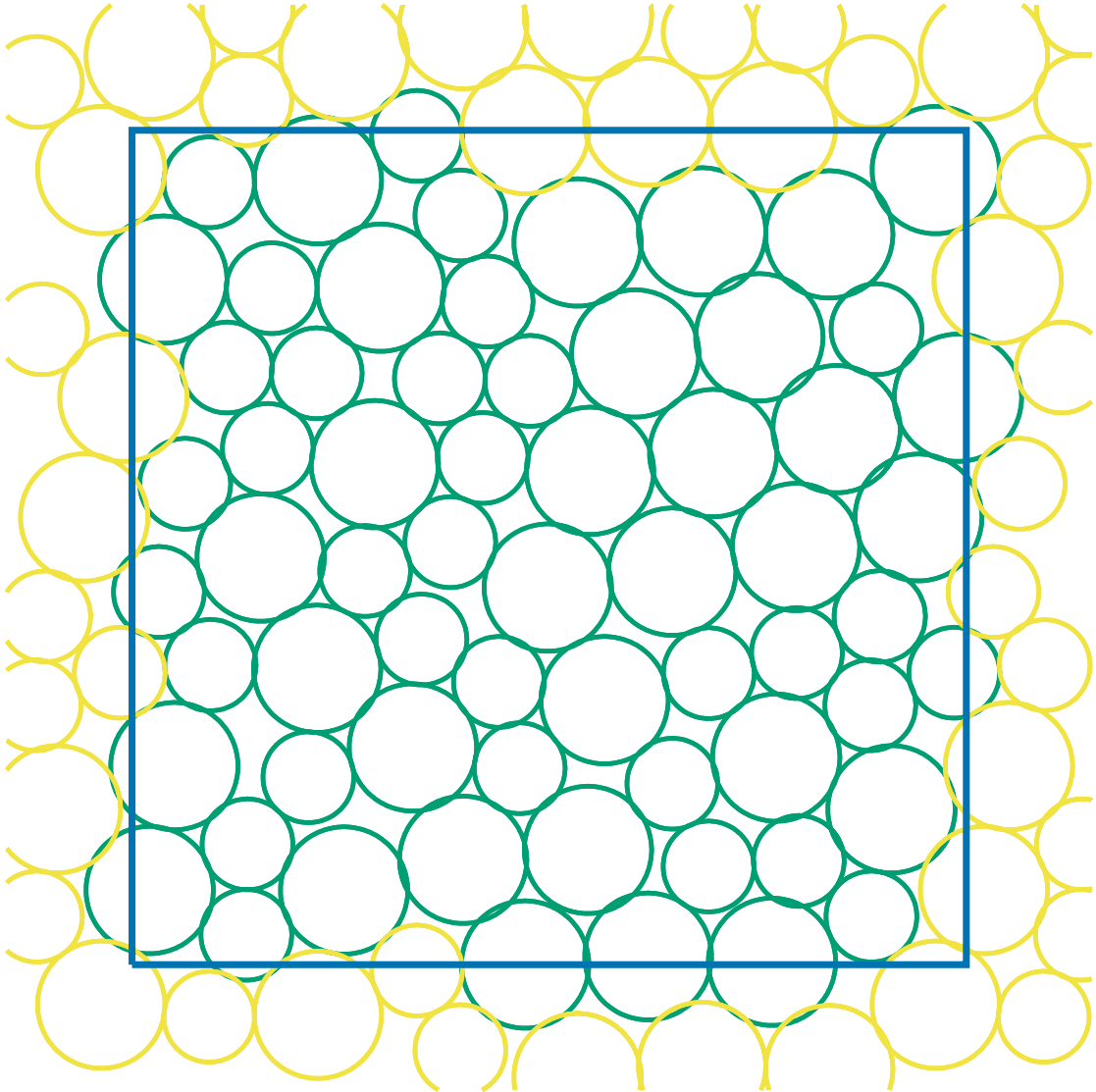

Jammed Packings: Contact Points

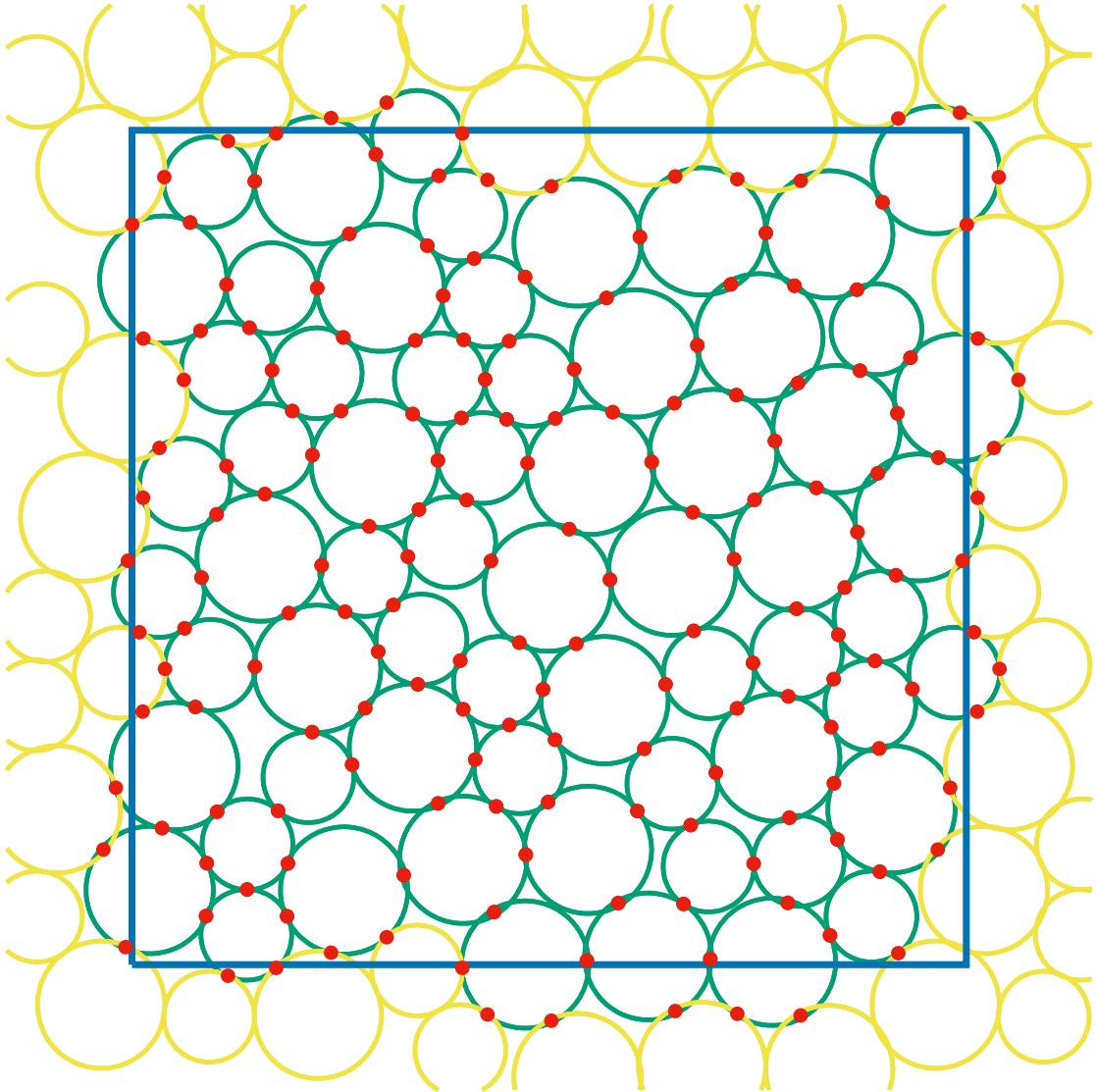

Summary

- We test the hypothesis of **equiprobability** for soft disks near the **unjamming transition**. Ref: S. Martiniani, K. J. Schrenk, K. Ramola, B. Chakraborty and D. Frenkel, Nature Physics (2017).
- We then analyze the system in a **fixed energy ensemble**.
- We develop a statistical framework for the transition using **local grain areas assigned to each contact** that play the role of "quasiparticles". Ref: K. Ramola and B. Chakraborty, Phys. Rev. Lett. 118, 138001 (2017).
- We use the **underlying distributions of interparticle distances** to derive a density of states of these areas.
- We show that to understand the scaling behaviour near the **unjamming transition**, one needs to account for **three-body interactions**.

Jammed Packings: Energy Landscape

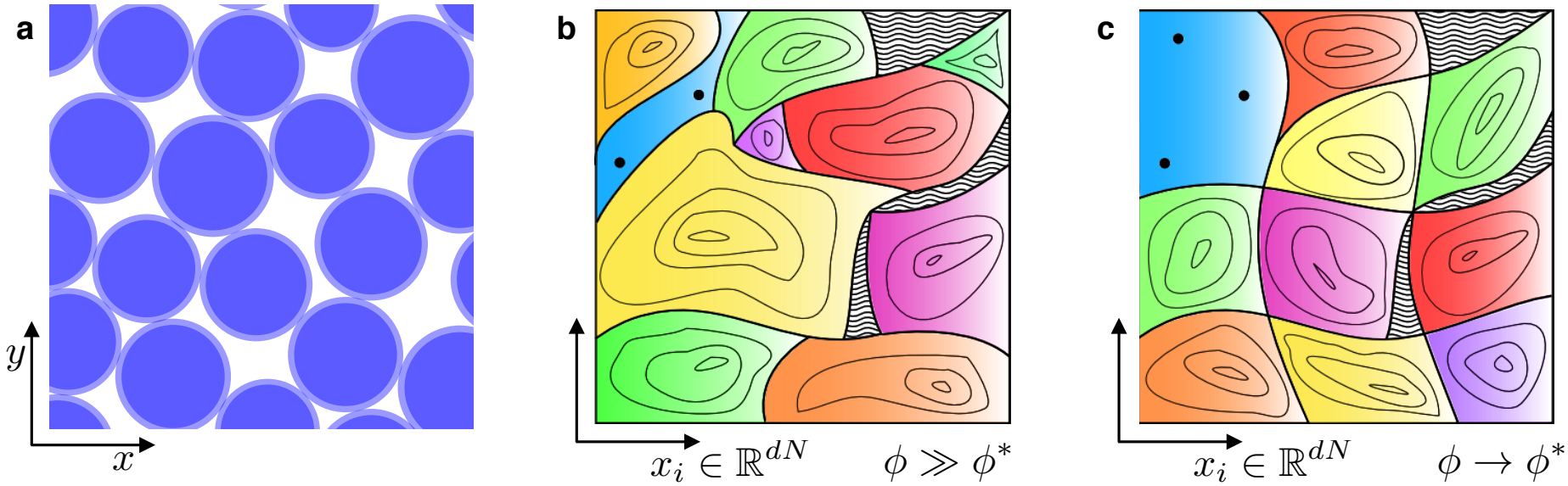

Figure: (a) Snapshot of a jammed packing of disks with a hard core (dark shaded regions) plus soft repulsive corona (light shaded regions). (b)-(c) Illustration of configurational space for jammed packings.

Numerical Simulations: Energy Functions

- We use a **soft potential** around a **hard core**

$$U(r) = \begin{cases} \infty & r \leq r_{\mathrm{HS}}, \\ 4\epsilon \left[\left(\dfrac{\sigma(r_{\mathrm{HS}})}{r^2 - r_{\mathrm{HS}}^2} \right)^{12} - \left(\dfrac{\sigma(r_{\mathrm{HS}})}{r^2 - r_{\mathrm{HS}}^2} \right)^{6} \right] + \epsilon & r_{\mathrm{HS}} < r < r_{\mathrm{SS}}, \\ 0 & r \geq r_{\mathrm{SS}} \end{cases} \tag{1}$$

- For short distances $r \to r_{SS}$ this becomes a **soft linear spring repulsion** potential of the form:

$$U(r) = \begin{cases} c_0 (r - r_{SS})^2 & r_{\mathrm{HS}} < r < r_{\mathrm{SS}}, \\ 0 & r \geq r_{\mathrm{SS}} \end{cases} \tag{2}$$

- We simulate **bidispersed** configurations (two different sizes of disks).

Global Variables approaching Jamming

- **Pressure**: $P \to 0^+$,
- **Energy**: $E_G \to 0^+$,
- **Packing Fraction**: $\phi \to 0.84...$,
- **Coordination number**: $\Delta Z = (Z - Z_{\text{iso}}) \to 0$,

$Z_{\text{iso}} = 2d \quad \to \quad \mathbf{4} \ \text{for} \ \ d = 2.$

Testing the Edwards Conjecture

- We performed a **direct test of the Edwards conjecture**, by numerically computing basin volumes of distinct jammed states (energy minima) of $N = 64$, frictionless disks held at a constant packing fraction ϕ.
- We compute Ω, **the number of distinct jammed states**, and the individual probabilities $p_{i \in \{1,\ldots,\Omega\}}$ of each observed packing to occur.
- The energy minimization procedure finds individual stable packings with a **probability** p_i **proportional to the volume** v_i of their basin of attraction.
- We compute v_i using a **thermodynamic integration scheme**, and compute the average basin volume $\langle v \rangle(\phi)$.

Phase Space Volumes

- The **number of jammed states** is, explicitly,

$$\Omega(\phi) = V_J(\phi)/\langle v \rangle(\phi), \tag{3}$$

  where $V_J(\phi)$ is the total available phase space volume at a given ϕ.
- A convenient way to check equiprobability is to **compare the Boltzmann entropy**

$$S_B = \ln \Omega - \ln N! \tag{4}$$

  which counts all packings with the same weight, and
- The **Gibbs entropy**

$$S_G = -\sum_i^{\Omega} p_i \ln p_i - \ln N! \tag{5}$$

- The Gibbs entropy satisfies $S_G \leq S_B$, **saturating the bound** when all p_i are equal: $p_{i \in \{1,\ldots,\Omega\}} = 1/\Omega$.

Characterizing Basin Volume Distributions

- We analyse the statistics of v_i **along with the pressure** P_i of each packing.
- It is convenient to study $F_i \equiv -\ln v_i$ as a function of $\Lambda_i \equiv \ln P_i$.
- This yields a linear relationship Ref: S. Martiniani, K. J. Schrenk, J. D. Stevenson, D. J. Wales, D. Frenkel, Phys. Rev. E 93, 012906 (2016).

$$\begin{aligned} \langle f \rangle_{\mathcal{B}}(\phi;\Lambda) =& \lambda(\phi)\Lambda + c(\phi) \\ =& \lambda(\phi)\Delta\Lambda + \langle f \rangle_{\mathcal{B}}(\phi) \ , \end{aligned} \tag{6}$$

  where $f = F/N$, and $\Delta\Lambda = \Lambda - \langle \Lambda \rangle_{\mathcal{B}}(\phi)$.

- The slope $\lambda(\phi)$ **characterizes the approach** to equiprobability.

Basin Volume Distributions

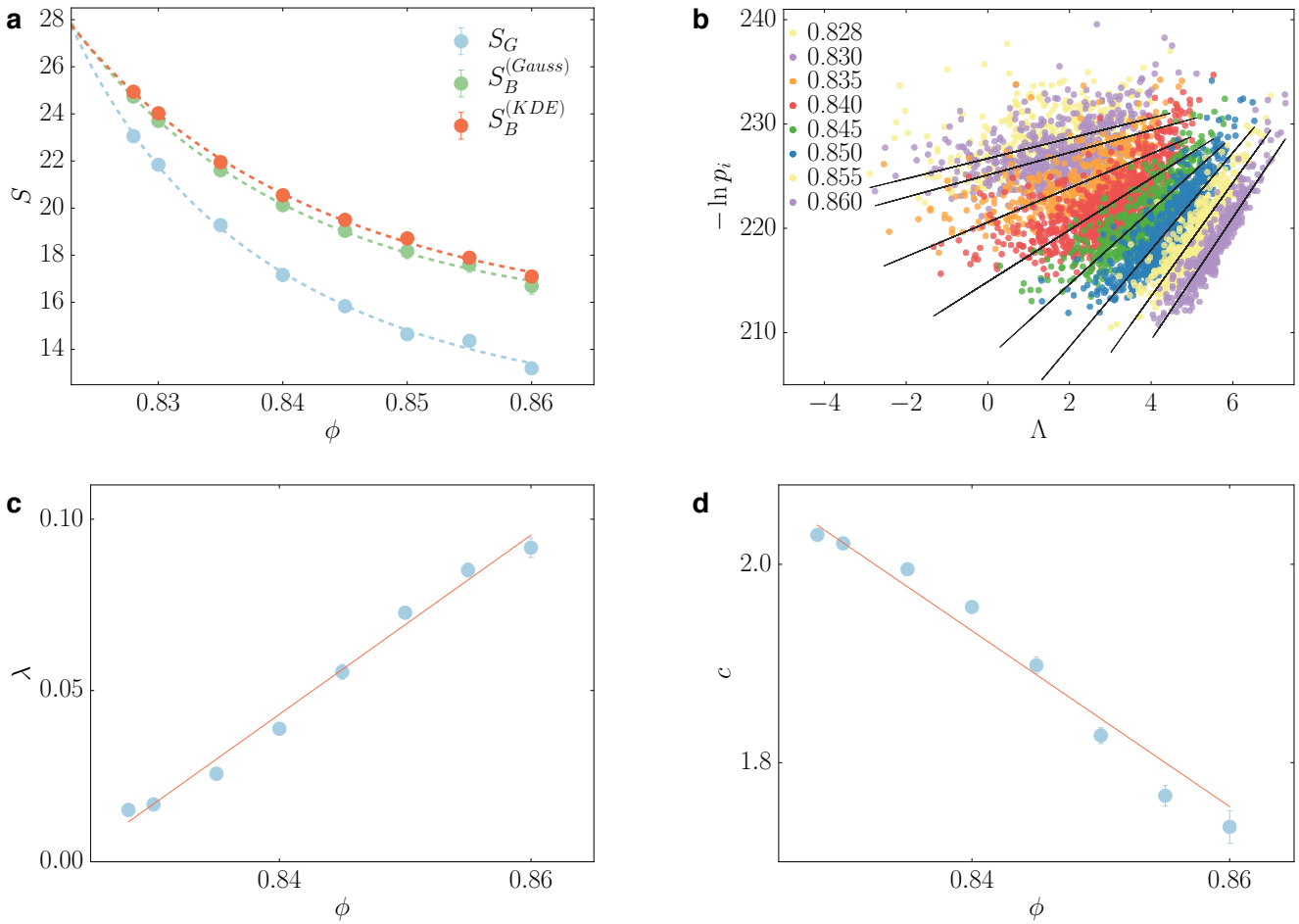

Figure: (a) Gibbs entropy S_G and Boltzmann entropy S_B. (b) Scatter plot of the negative log-probability of observing a packing, $-\ln p_i = F_i + \ln V_J(\phi)$.

Jammed Packings: Minimum Cycle Basis

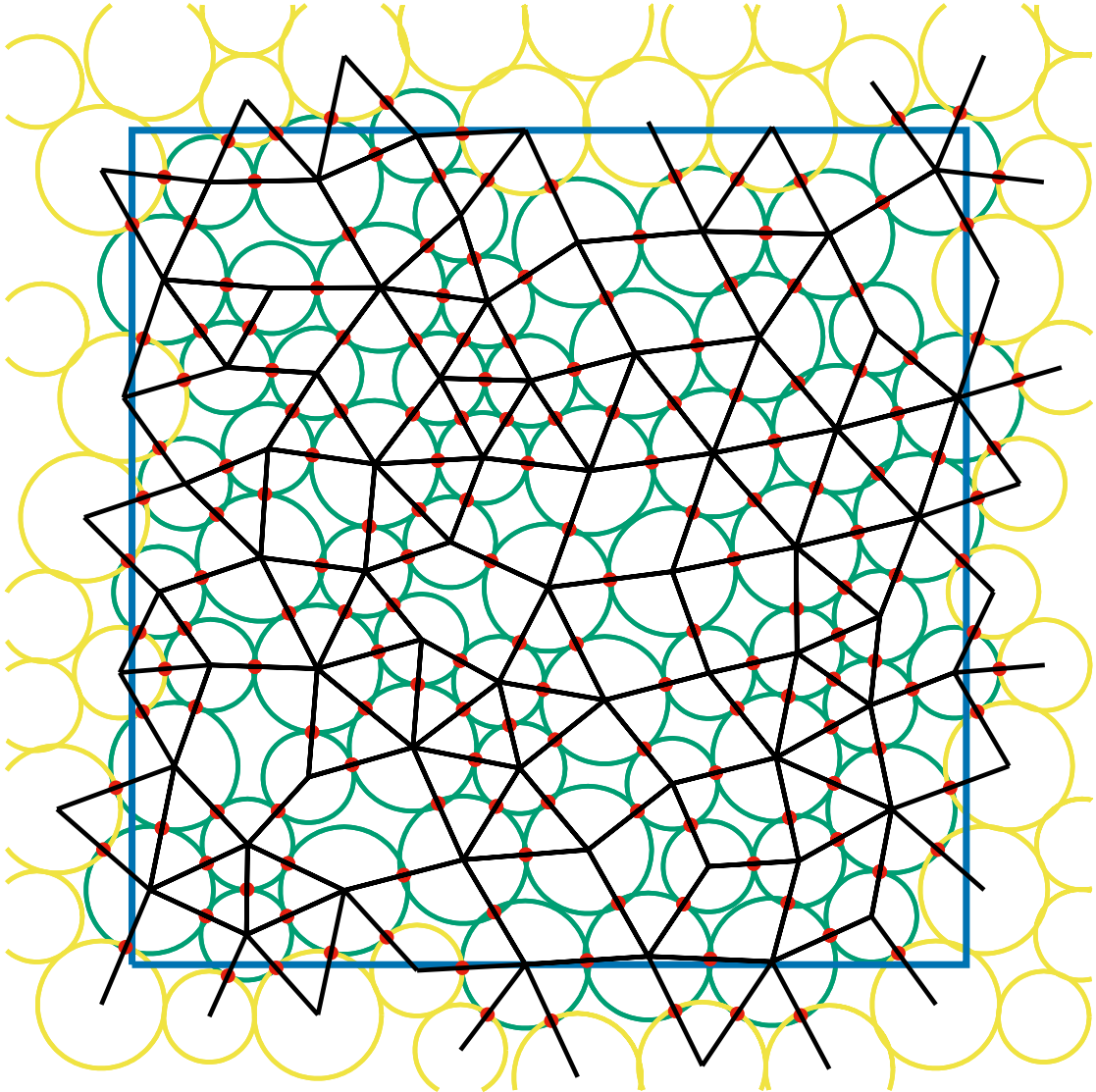

Partition Function

- The partition function at a fixed energy E_G is given by

$$\Omega(E_G) = \int \mathcal{D}[\{\vec{r}_g, \sigma_g\}] \delta\left(E_G - V[\{\vec{r}_g, \sigma_g\}]\right) \delta\left(\frac{\partial V[\{\vec{r}_g, \sigma_g\}]}{\partial \vec{r}_g}\right). \tag{7}$$

- Jammed states are characterised by a **system spanning contact network**.
- For **frictionless disks** this naturally partitions the space into **convex minimum cycles** (or faces) of z_v sides each.
- The **loop constraints** around each face can be implemented as

$$\{\vec{r}_g\} \to \{\vec{r}_{g,g'}\} \times \prod_v \delta\left(\sum_{i=1}^{z_v} \vec{r}^{\,i}_{g,g'}\right), \quad \text{with} \quad \vec{r}_{g,g'} = \vec{r}_{g'} - \vec{r}_g. \tag{8}$$

Jammed Packings: Grain Polygons and Void Polygons

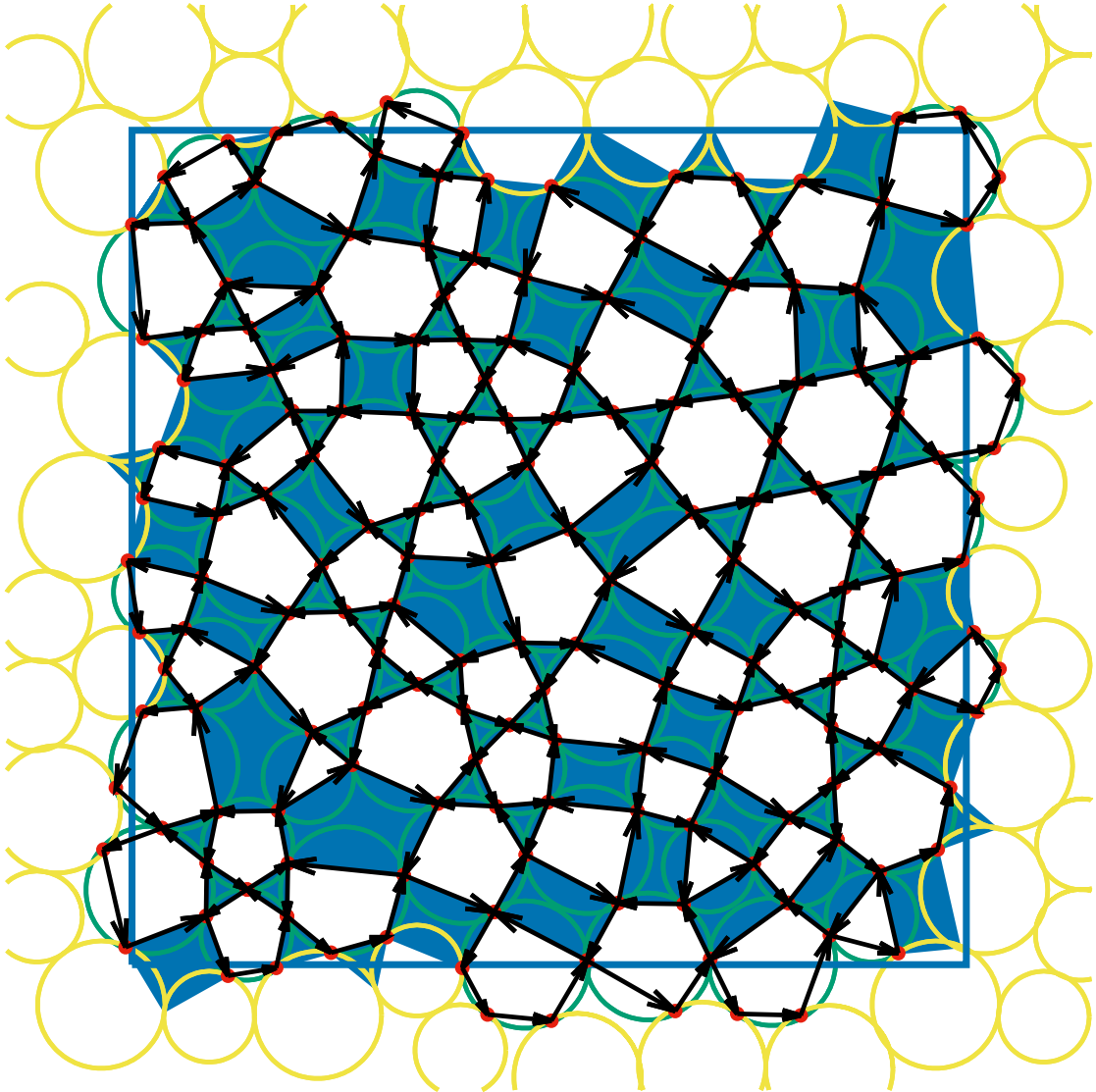

Total Grain Area

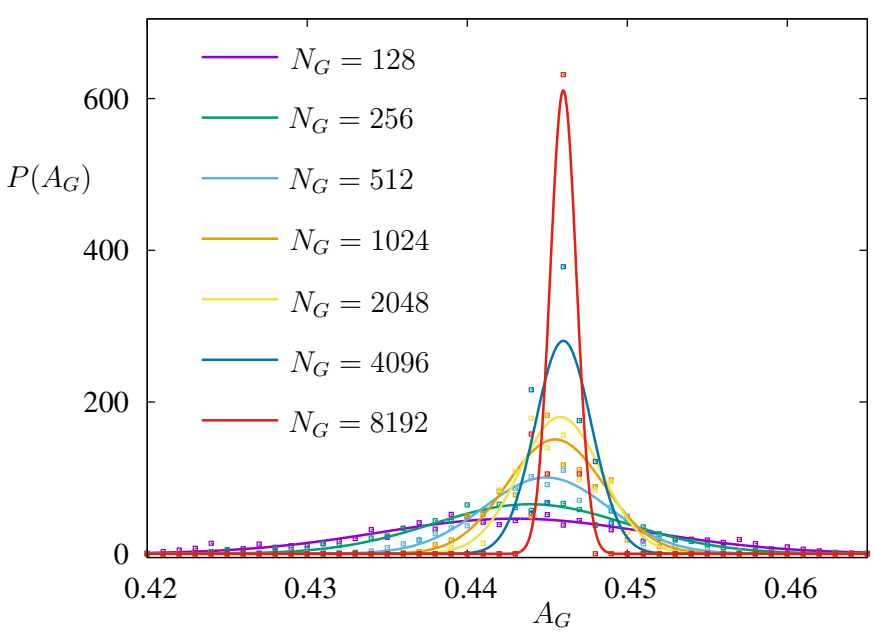

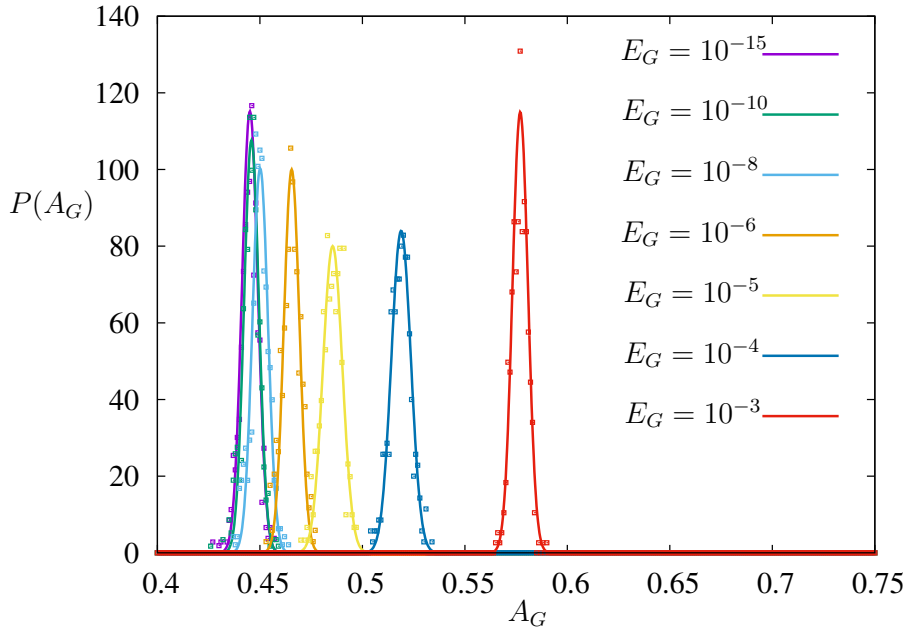

Figure: **(Left)** Distribution of the total area covered by the grain polygons A_G at $E_G = 10^{-15}$. Using finite-size scaling fits we find is $A_G^* = 0.446(1)$ as the number of grains $N_G \to \infty$ and $E_G \to 0^+$. **(Right)** Behaviour of the grain area distributions for different energies for packings of $N_G = 512$ disks.

Scaling with Energy

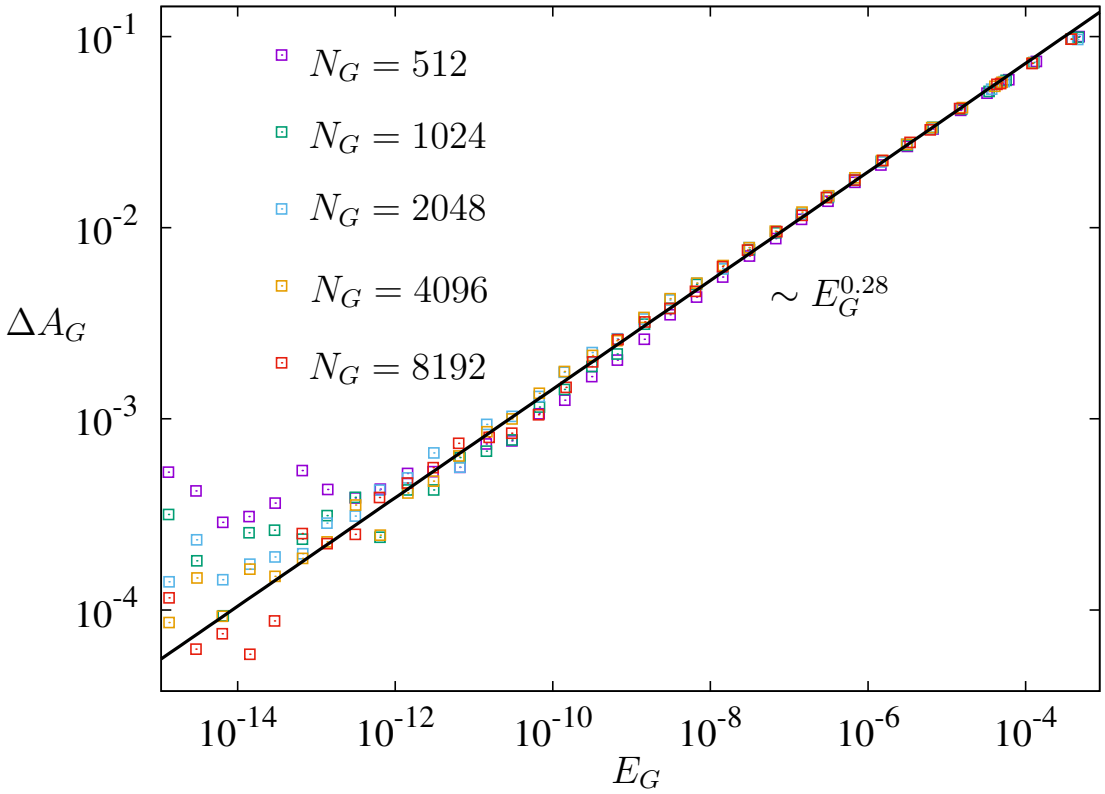

Figure: Scaling of the excess grain area $\Delta A_G = A_G - A_G^*$ with total energy per particle E_G. We find that the excess grain area scales as a power of the total energy in the system with exponent $\beta_E = 0.28(2)$.

Scaling with Coordination

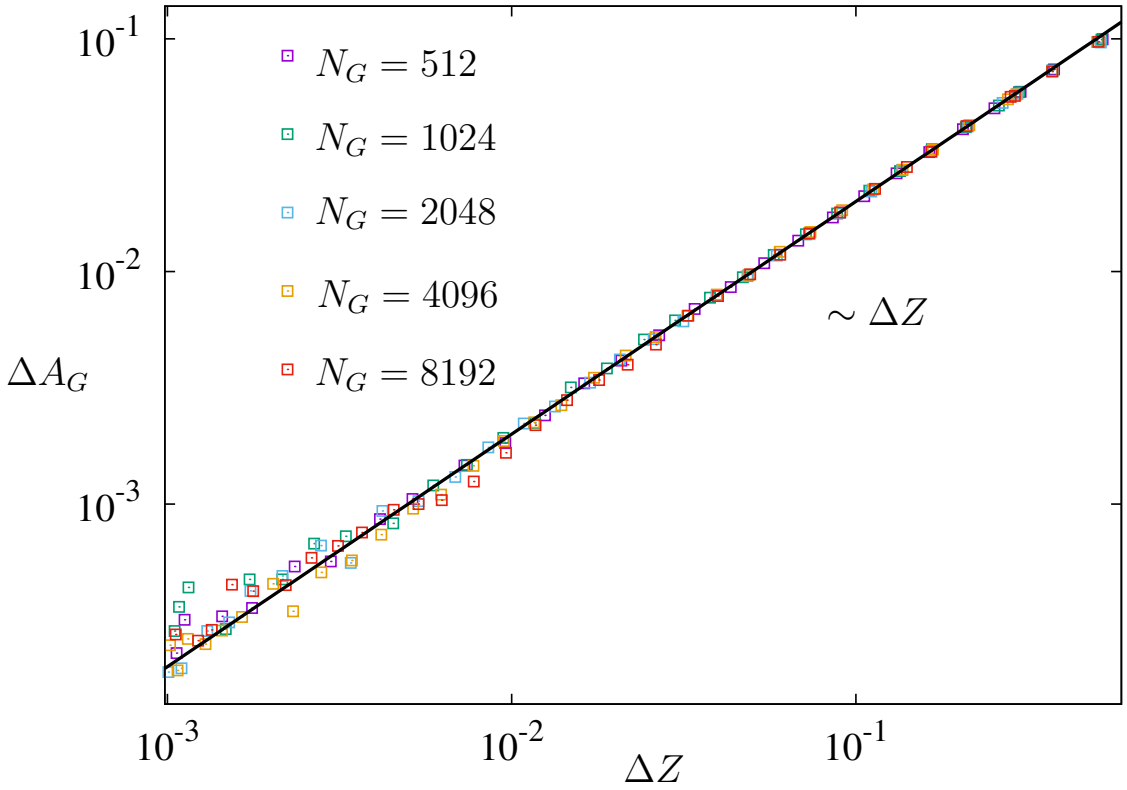

Figure: Scaling of ΔA_G with excess coordination in the system ΔZ. We find that the excess grain area scales as a power of ΔZ with exponent $\beta_Z = 1.00(1)$.

Edge Triangles and Local Areas

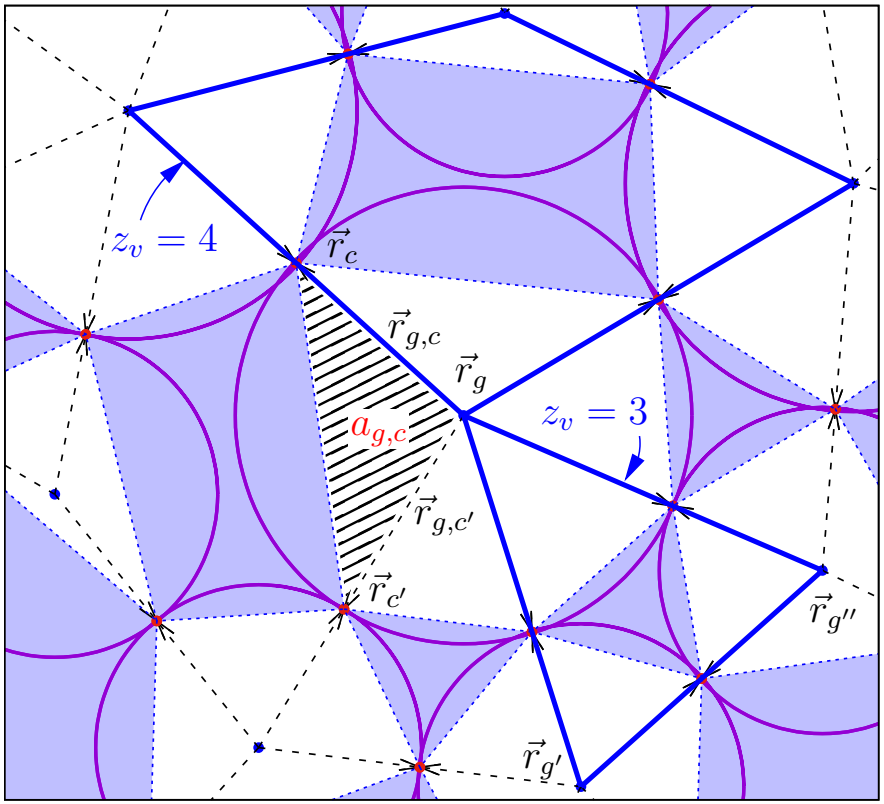

Figure: A section of a jammed configuration of soft frictionless disks. The centers of the grains with radii $\{\sigma_g\}$ are located at positions $\{\vec{r}_g\}$. The triangle formed by the points $(\vec{r}_g, \vec{r}_c, \vec{r}_{c'})$ (shaded area) is uniquely assigned to the contact c and has an associated area $a \equiv a_{g,c}$, with a normalized area $\alpha_c = a_{g,c}/\sigma_g^2$.

Partition Function and Local Distributions

- These basic triangular units are the **local measure of density (packing fraction)** in our description:

$$\alpha_e = \frac{a_{g,e}}{\sigma_g^2} \quad \in \quad \left[0, \frac{1}{2}\right]. \tag{9}$$

- We can express the partition function in terms of the **joint density of states** of these local areas

$$\Omega(E_G, N_C) = \left(\prod_{i=1}^{N_C} \int_0^{1/2} d\alpha_i \right) g_{E_G}(\alpha_1, \alpha_2, ..., \alpha_{N_C}). \tag{10}$$

- Similarly we can compute probability distributions

$$p_{E_G}(\alpha_1) = \left(\prod_{i=2}^{N_C} \int_0^{1/2} d\alpha_i \right) \frac{g_{E_G}(\alpha_1, \alpha_2, ..., \alpha_{N_C})}{\Omega(E_G, N_C)}. \tag{11}$$

- In real systems (and simulations), the number of contacts N_C **is a fluctuating quantity**.

Local Area Distribution

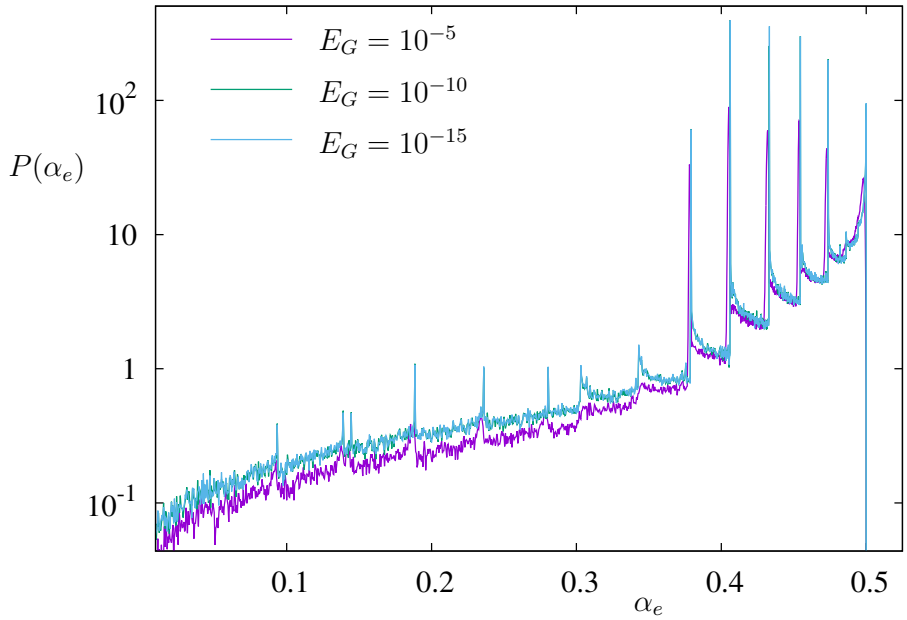

Figure: Distribution of areas of the edge triangles $\alpha_e = a_{g,e}/\sigma_g^2$ for $N_G = 2048$. $\alpha_e \to 1/2$ corresponds to disks with relative contact angles close to $\pi/2$. We find **well defined peaks that get sharper as** $E_G \to 0^+$.

Ordered Structures

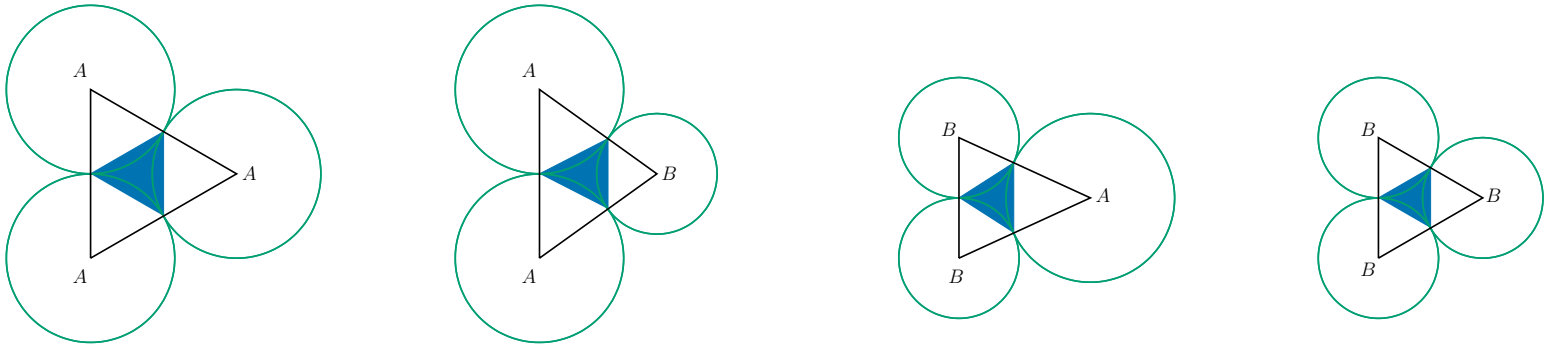

Figure: The four **three-disk crystallization configurations** that can occur in bidispersed systems. This causes ordered peaks to appear in the distribution of edge triangle areas (white triangles). The fraction of the system in these ordered structures gives us a **measure of order** in the system.

- We **focus on the** $A - A - A$ **case**. The generalization to the polydisperse case is straightforward.

Building a Theory

- We use the distribution of contact lengths to derive the areas, **which relates them to the energy**.
- The distribution of individual areas is given by

$$p(a) = \int d\vec{r}_1 \int d\vec{r}_2 \; p(\vec{r}_1, \vec{r}_2) \; \delta \left(\frac{|\vec{r}_1 \times \vec{r}_2|}{2} - a \right). \tag{12}$$

  where $\vec{r}_1$ and $\vec{r}_2$ are the contact vectors bounding the triangle.
- The one point distribution is **independent of orientation**

$$p(\vec{r}_1) = \int d^2\vec{r}_2 p(\vec{r}_1, \vec{r}_2) = \frac{1}{2\pi} p(|\vec{r}_1|). \tag{13}$$

- The **joint distribution** can be decomposed as

$$p(\vec{r}_1, \vec{r}_2) = p(|\vec{r}_1|)p(|\vec{r}_2|)p(\sin\theta). \tag{14}$$

Local Areas

- In terms of the **scaled distances** $\vec{r} \to \vec{r}/\sigma_g$ we have

$$P(\alpha) = \int_0^1 dr_1 \int_0^1 dr_2 \int_0^1 d\sin\theta \; P(r_1)P(r_2)P(\sin\theta) \; \delta\left(\frac{1}{2} r_1 r_2 \sin\theta - \alpha\right). \tag{15}$$

- $\alpha < 1/2$ combined with the delta function **produces a singularity** in $p(\alpha)$ as $r_1 \to 1$, $r_2 \to 1$ and $\theta \to \pi/2$.

- Therefore **the relative angle between contact vectors is crucial** in determining the nature of the divergence as $E_G \to 0^+$.

Observed Underlying Distributions

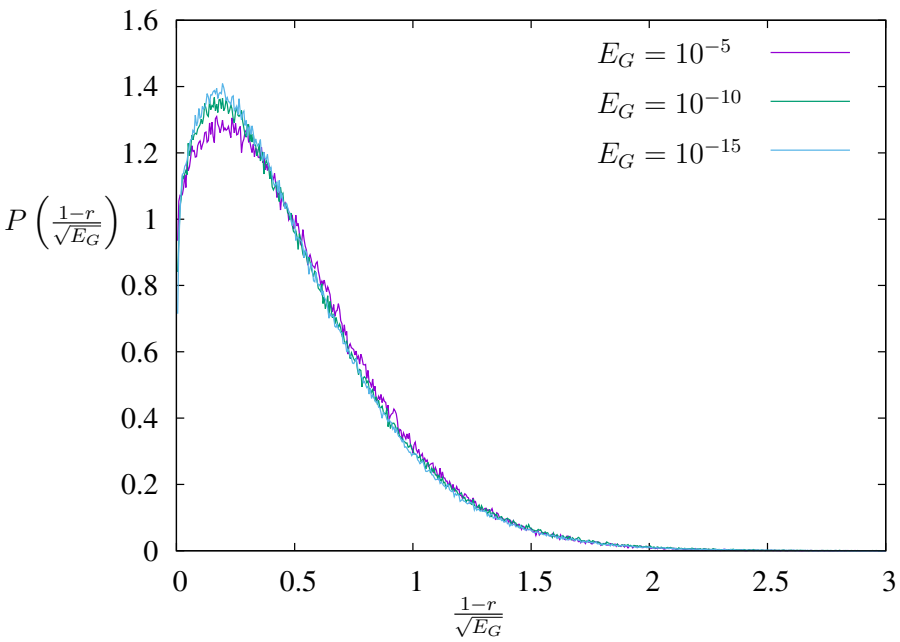

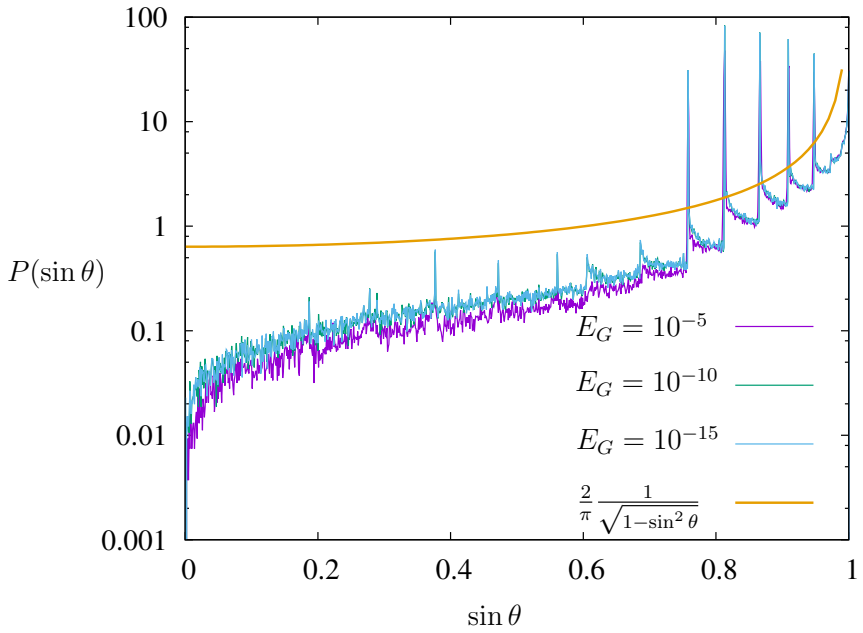

Figure: **(Left)** Distribution of lengths of contact vectors measured in packings with $N_G = 2048$ at different energies. The plot shows the distribution of $(1-r)/\sqrt{E_G}$, where $r = |\vec{r}_{g,c}|/\sigma_g$. **(Right)** Distribution of relative contact angles $\theta = \theta_{g,c'} - \theta_{g,c}$.

Underlying Distributions: Contact Vector Lengths

- Contact lengths are **fluctuating quantities**

$$|\vec{r}| = \sigma_g - \Delta r \quad \text{with} \quad 0 < \Delta r < \sigma_g \tag{16}$$

- For linear spring potentials

$$E_G = \frac{1}{N_G} \sum_{i=1}^{N_C} (\Delta r_i)^2 \tag{17}$$

- Therefore the contact fluctuations are drawn from a **distribution with an energy dependent width** $\sqrt{E_G}$

$$p\left(\Delta r = \frac{|\vec{r}|}{\sigma_g} - 1\right) = \frac{1}{\sqrt{E_G}} \mathcal{P}\left(\frac{\Delta r}{\sqrt{E_G}}\right) \tag{18}$$

- This is **independent of the cycle** to which it belongs

Building the Angular Distributions

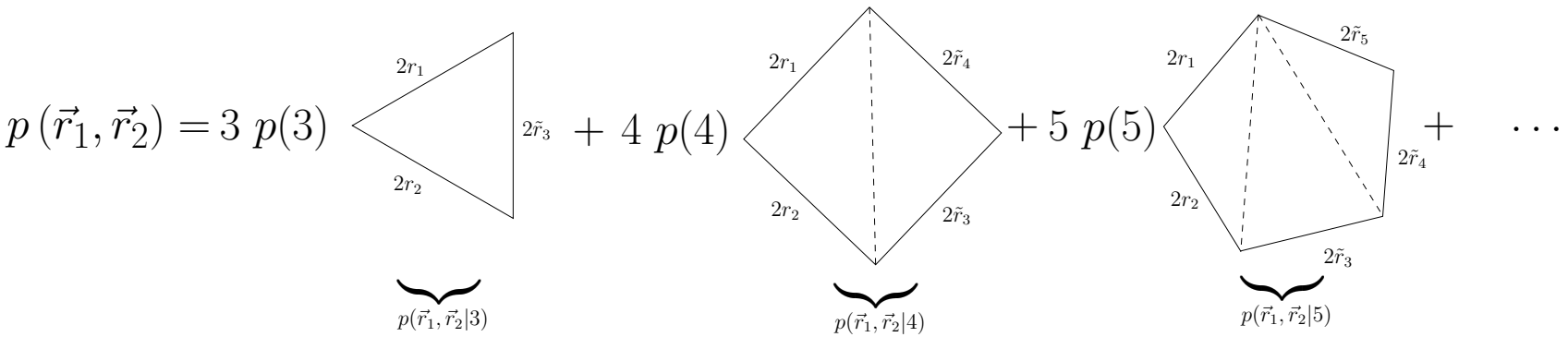

Figure: Diagrams appearing in the expansion for the joint distribution $p(\vec{r}_1, \vec{r}_2)$. The vectors $\tilde{r}$ are integrated over.

- The terms corresponding to $z_v = 3$ have a fixed length for all the sides as $E_G \to 0^+$, and therefore give rise to $\rho(\theta)$ **localized around a single value** $\theta = \arcsin \frac{\sqrt{3}}{2}$.
- The terms corresponding to $z_v > 3$ **have unconstrained sides** (depicted with dashed lines) and therefore contribute a finite amount to $\rho(\theta)$ at $\theta = \pi/2$.

Angular Distributions: > 3-minimum Cycles

- For $z_v > 3$ we have a **finite expansion about** $\theta = \pi/2$

$$p(\theta, > 3) = \frac{2}{\Delta} p(\pi/2) \quad \text{for} \quad \left|\theta - \frac{\pi}{2}\right| < \Delta \tag{19}$$

- Changing variables $\theta \to \sin\theta$

$$p(\sin\theta, > 3) = \frac{2p(\pi/2)}{\Delta\sqrt{1 - \sin^2\theta}} \quad \text{for} \quad \left|\theta - \frac{\pi}{2}\right| < \Delta \tag{20}$$

- We refer to the divergence in the area distribution arising from $\theta \to \pi/2$ as *disordered divergences*.

Angular Distributions: 3-minimum Cycles

- For $z_v = 3$ we have a distribution **centered at a finite value**

$$p(\theta, 3) \sim \frac{1}{\sqrt{E_G}} \mathcal{P}\left(\frac{\theta - \arcsin \frac{\sqrt{3}}{4}}{\sqrt{E_G}} \right). \tag{21}$$

- Changing variables $\theta \to \sin\theta$

$$p(\sin\theta, 3) \sim \frac{1}{\sqrt{1 - \sin^2\theta}} \frac{1}{\sqrt{E_G}} \tilde{\mathcal{P}}\left(\frac{\sin\theta - \frac{\sqrt{3}}{4}}{\sqrt{E_G}} \right). \tag{22}$$

- The contribution at $\theta = \pi/2$ is **exponentially suppressed**.
- This leads to an **integrable singularity** for the probability of areas.
- We refer to these as *ordered divergences*.

Ordered and Disordered Distributions

- We can **split the distribution into two classes** as follows

$$p(\alpha) = \frac{g(\alpha)}{N_C} = p(\alpha, 3) + \underbrace{p(\alpha, > 3)}_{p_{DO}(\alpha)+p_{\mathrm{reg}}(\alpha)} , \tag{23}$$

- with

$$p(3) = \int_0^{1/2} p(\alpha, 3) d\alpha, \qquad n(3) = N_C p(3), \tag{24}$$

- and

$$p(> 3) = \int_0^{1/2} p(\alpha, > 3) d\alpha, \qquad n(> 3) = N_C p(> 3). \tag{25}$$

Scaling Form

- The disordered divergence has the following **scaling form**

$$p_{DO}(\alpha) = {E_G}^{-1/4} \mathcal{P}_{DO}\left(\frac{\frac{1}{2} - \alpha}{\sqrt{E_G}}\right). \tag{26}$$

- which possesses the following **asymptotic behaviour**

$$\mathcal{P}_{DO}(x) \sim \begin{cases} x^{3/2}\ , \ x \to 0, \\ \\ x^{-1/2}\ , \ x \to \infty\ . \end{cases} \tag{27}$$

- Similarly we find that the "ordered" distribution has a scaling form

$$p(\alpha, 3) = {E_G}^{-1/2} \mathcal{P}_{O}\left(\frac{\frac{\sqrt{3}}{4} - \alpha}{\sqrt{E_G}}\right), \tag{28}$$

- which is **integrable in the** $E_G \to 0^+$ **limit**.

Scaling Collapse

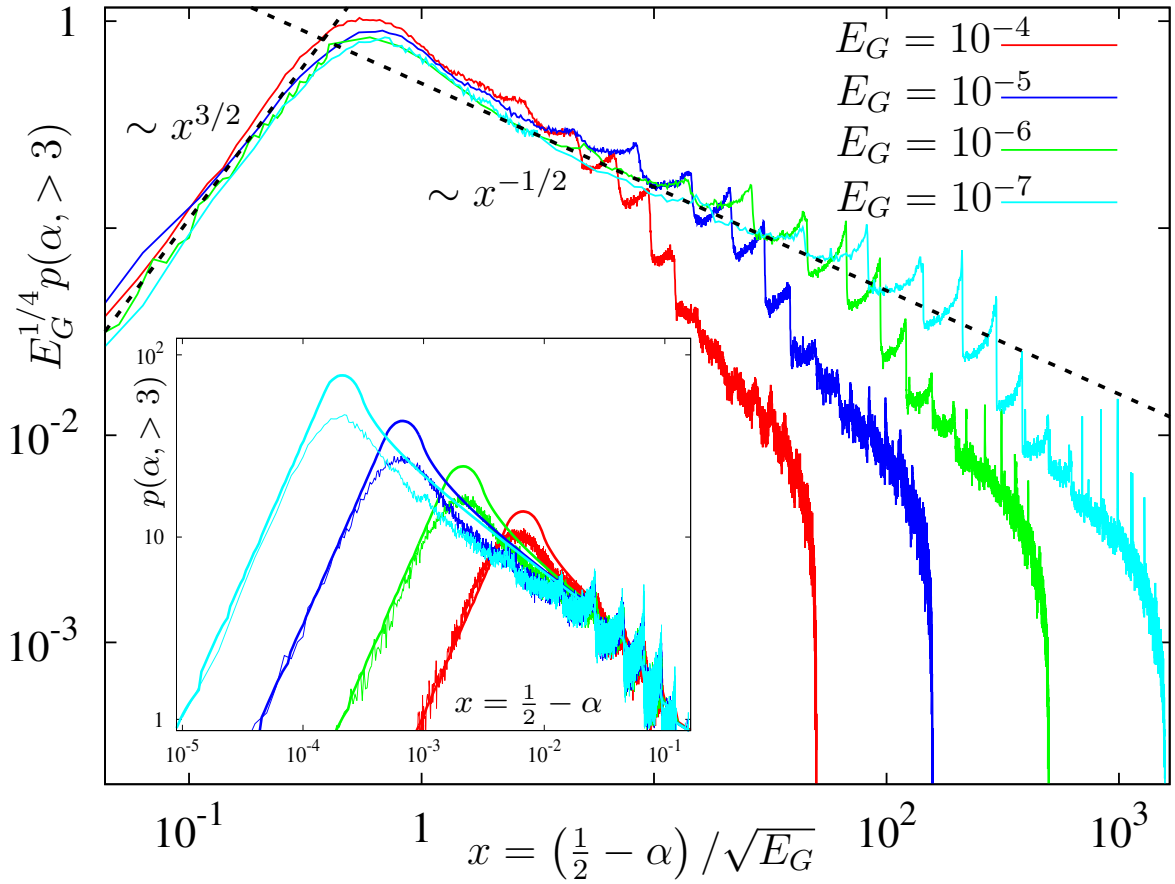

Figure: Scaling collapse of the distribution of areas $p(\alpha, > 3)$ of the $z_v > 3$ cycles at different energies.

Scaling Collapse

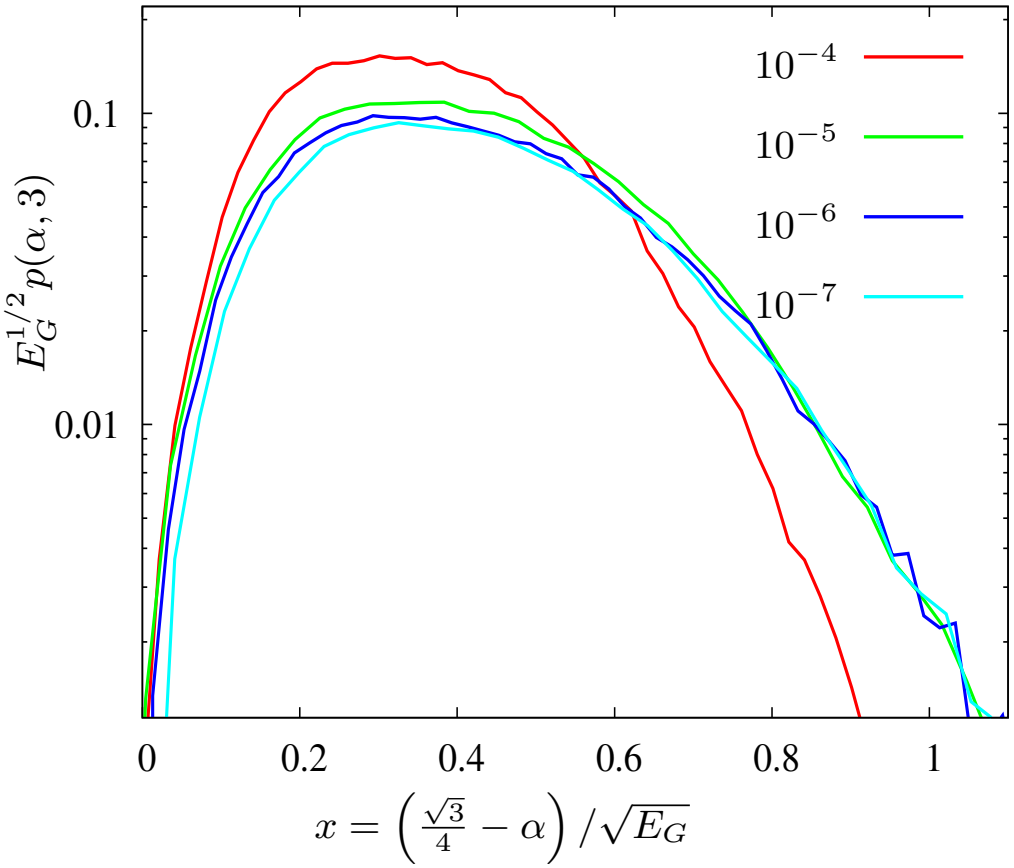

Figure: Scaling collapse of the distribution of areas of the ordered ($z_v = 3$) cycles $p(\alpha, 3)$.

Global Scaling

- The **overall density of states** is given by

$$g(\alpha) = N_C \left(p(\alpha, 3) + p(\alpha, > 3) \right), \tag{29}$$

with

$$p(\alpha, > 3) = p_{\text{reg}}(\alpha) + \underbrace{p_{DO}(\alpha)}_{\Delta E^{-1/4}}. \tag{30}$$

- The **regularity of** $g(\alpha)$ **at** $E_G = 0$ leads to

$$N_C = \frac{\int_0^{1/2} g_{\text{reg}}(\alpha) d\alpha}{p(\alpha, > 3) - \Delta}. \tag{31}$$

- Which implies the **scaling of the excess coordination**

$$\Delta Z \sim E^{1/4}. \tag{32}$$

Comparision with Simulations

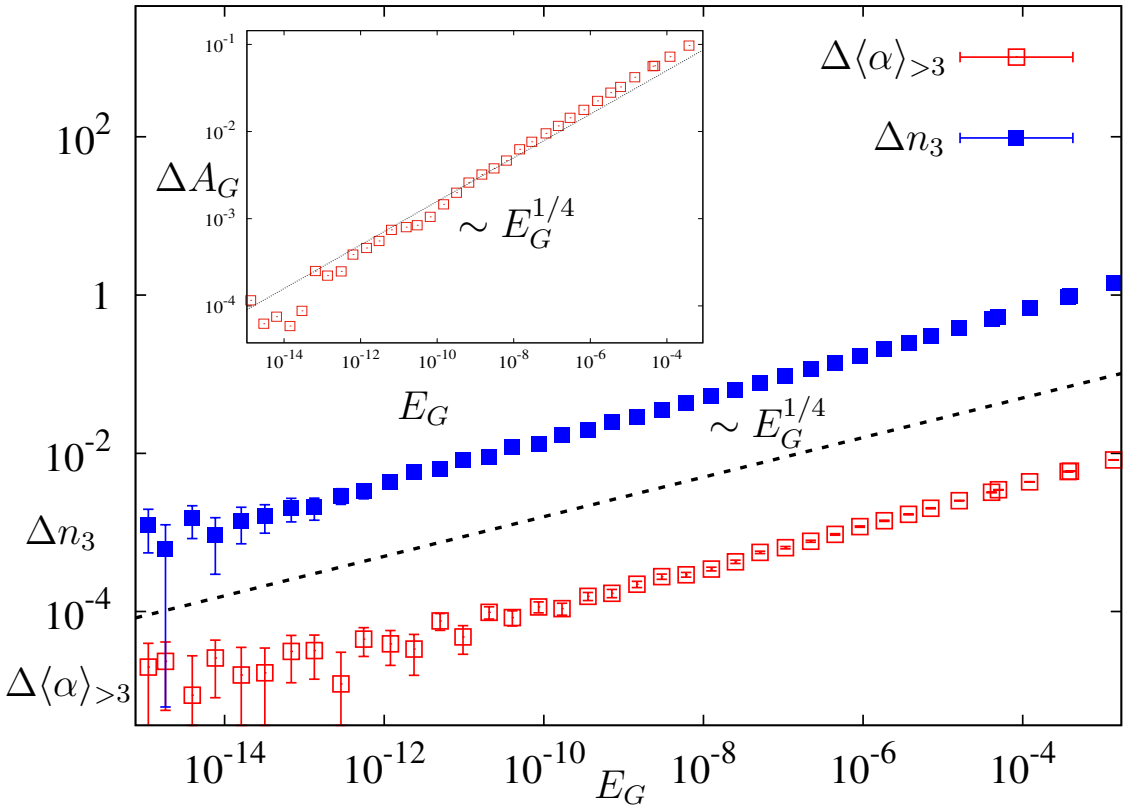

Figure: Scaling of global quantities: (i) the excess number of contacts in the $z_v = 3$ cycles ($\Delta n_3 = n_3(E_G) - n_3(0)$) (ii) the excess normalized area per contact of the $z_v > 3$ cycles ($\Delta\langle\alpha\rangle_{>3} = \langle\alpha\rangle_{>3}(E_G) - \langle\alpha\rangle_{>3}(0)$).

Different Repulsive Potentials

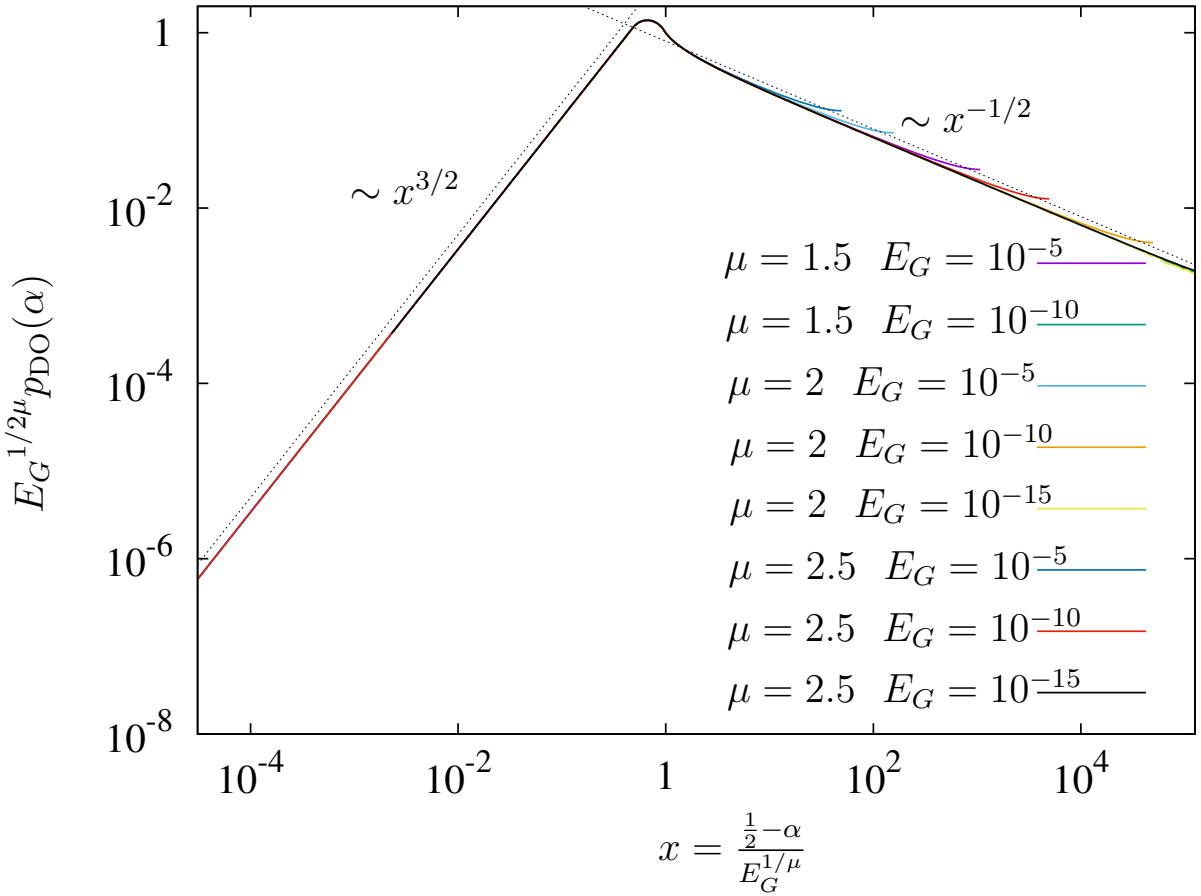

Figure: Scaling collapse of the theoretical distribution for different repulsive potentials $\mu = 1.5, 2$ and 2.5 at varying global energies.

Conclusions

- We numerically tested the **equiprobability of jammed configurations** near the unjamming transition of soft disks.
- We developed a **statistical framework for the transition** in two dimensions.
- We used **local grain areas assigned to each contact** as the microscopic degrees of freedom with which to describe the system.
- We found that large scale **numerical simulations match the predictions** very well.
- It would be interesting to extend this analysis to systems with **different shapes of particles** and **frictional systems**.

Thank You.